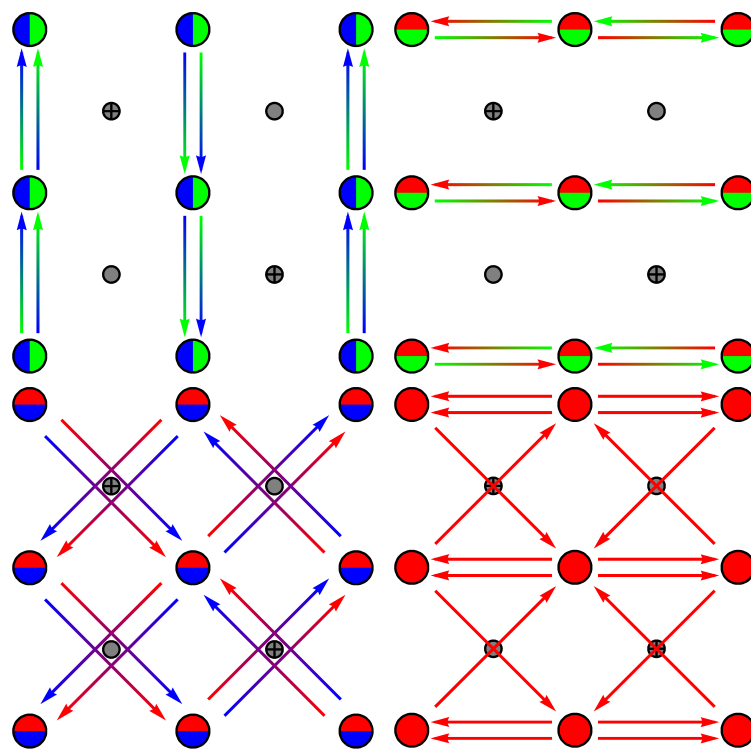


Another thesis on SNS junctions: numerical simulations and calculations



Master's Thesis

by

Umut Nefta Kanilmaz

Submission date: 25. February 2018

Advisor: PD Dr. Igor Gornyi
Co-Advisor: Prof. Dr. Alexander Mirlin

Ich erkläre hiermit, dass die Arbeit selbstständig angefertigt, alle benutzten Quellen und Hilfsmittel vollständig und genau angegeben und alles kenntlich gemacht wurde, das aus Arbeiten anderer unverändert oder mit Abänderungen entnommen ist.

Karlsruhe, den 24. Januar 2017

.....
(**Alexander Gawrilow**)

Contents

1	Things you have to know before you read my thesis...	1
2	Analytical Model	3
2.1	Foundation of the quasiclassical model	3
2.2	Plane setup: calculation of current	4
2.3	Calculation of QPC current	6

1 Things you have to know before you read my thesis...

The interface between a superconductor and a normal metal can be described with an effective 1D Bogoliubov-de-Gennes Hamiltonian, describing the superconducting order parameter with a step-like function as order parameter

$$\begin{pmatrix} -\frac{\hbar^2}{2m}\nabla^2 - \epsilon_F & \Delta(x) \\ \Delta^*(x) & \frac{\hbar^2}{2m}\nabla^2 + \epsilon_F \end{pmatrix} \begin{pmatrix} u(x) \\ v(x) \end{pmatrix} = E \begin{pmatrix} u(x) \\ v(x) \end{pmatrix}, \quad \Delta(x) = \Delta_0 e^{i\phi\theta(x)} \quad (1.1)$$

This is the so called Blonder-Tinkham-Klapwijk model and can be solved separately for each of side of the NS interface. For the N side, the superconducting order parameter vanishes and the equation leads to two solutions

$$\psi_e^\pm(x) = \begin{pmatrix} 1 \\ 0 \end{pmatrix} e^{\pm i k_e x}, \quad k_e = k_F \sqrt{1 + \frac{E}{e_F}} \quad (1.2)$$

$$\psi_h^\pm(x) = \begin{pmatrix} 0 \\ 1 \end{pmatrix} e^{\pm i k_h x}, \quad k_h = k_F \sqrt{1 - \frac{E}{e_F}} \quad (1.3)$$

TODO: electron solution because of term $e_f + E$, hole solution because of $e_f - E$?

2 Analytical Model

This chapter intends to explain the calculation of the critical current in different SNS junctions. For this purpose, a quasiclassical transport theory is used and its foundations are explained in the first section. This technique is then employed for a clean SNS junction and an expression for the Josephson current is found. In the following section the calculations used for the clean setup are extended for the more sophisticated quantum point contact (QPC) and here as well, the current for the QPC-gated junction is found.

2.1 Foundation of the quasiclassical model

This section explains preliminary assumptions made to describe the current in a SNS junction. The aim is to express the current through the junction using a quasiclassical approach. Essentially, this means that the Andreev bound states are associated with straight trajectories connecting the superconducting leads. The superconducting current density is then expressed in terms of these trajectories.

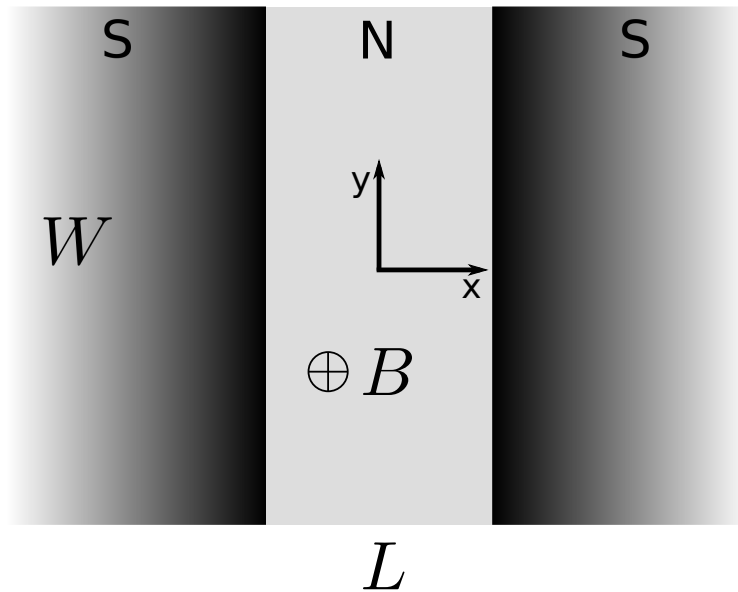


Figure 2.1: *Schematic representation of a short and wide SNS junction.*

The two dimensional junction, a schematic is shown in fig 2.1, is a short and wide junction

with width W and length L , where $W \gg L$. The NS-interfaces are parallel to the y -axis and are placed at $x = \pm L/2$. Each of the superconducting leads has a phase χ_1 and χ_2 and the overall phase difference is $\chi = \chi_1 - \chi_2$. The superconducting gap parameter is only present in the superconducting leads and zero in the normal region and can be expressed as

$$\Delta(x) = |\Delta|e^{\chi_1}\Theta(-L/2 - x) + |\Delta|e^{\chi_2}\Theta(x - L/2) \quad (2.1)$$

We consider the low temperature limit, where the thermal length scale of the system is smaller larger than the sample length:

$$L_T = \hbar v_F / k_B T \gg L \quad (2.2)$$

The considered sample is ballistic, the fermi wavelength λ_F is smaller than the sample length L . It has the BCS coherence length $\zeta = \hbar v_F / \pi \Delta$, where ζ is much larger than the Fermi velocity $\zeta \gg v_F$ **TODO: (in order to induce superconductivity in the system?)**. The relation between the coherence length ζ and the sample length L determines, if the considered junction is a *short* or a *long* junction:

$$\begin{aligned} \zeta \ll L &\rightarrow \text{long junction} \rightarrow \text{many Andreev levels} \\ \zeta \gg L &\rightarrow \text{short junction} \rightarrow \text{one Andreev level} \end{aligned}$$

TODO: replace equation above with good picture (E ; delta, andreec levels...)

The presence of magnetic field in the normal region of the sample will lead to a bending of the trajectories due to the Lorentz force. Depending on the strength of magnetic field B and the Fermi velocity the radius of this curve is

$$r_B = \frac{m^* v_F}{eB} \quad (2.3)$$

In order to justify the assumption of straight trajectories, either the magnetic field has to be weak enough or the Fermi velocity (wavelength) has to be large (short) enough. Then, the cyclotron radius r_B is larger than the sample size L and straight trajectories are a valid assumption.

2.2 Plane setup: calculation of current

To derive the current for the SNS setup depicted in figure 2.1, we start by writing down the Bogoliubov-de-Gennes Hamiltonian for this system.

$$\begin{pmatrix} -\frac{\hbar^2}{2m}\nabla^2 - \epsilon_F & \Delta(x) \\ \Delta^*(x) & \frac{\hbar^2}{2m}\nabla^2 + \epsilon_F \end{pmatrix} \begin{pmatrix} \psi_e \\ \psi_h \end{pmatrix} = E \begin{pmatrix} \psi_e \\ \psi_h \end{pmatrix} \quad (2.4)$$

The Hamiltonian above uses eq. (2.1) for the spatially dependent superconducting gap parameter $\Delta(x)$. The eigenvalue problem has two solutions

$$\epsilon_{\pm} = \frac{\hbar^2 k_{\pm}^2}{2m} = -\epsilon_F - \sqrt{E_k^2 - |\Delta|^2} \quad (2.5)$$

TODO: Hier fehlt die Herleitung für Wellenfunktionen, Ausdruck für den Strom etc.!

Current density for short and long junction limit: In the short junction limit the current density can be derived from the scattering matrix formalism and it reads

$$\mathcal{J}^s(\chi) = \frac{\mathcal{T} \sin \chi}{\sqrt{1 - \mathcal{T} \sin^2 \frac{\chi}{2}}} \quad (2.6)$$

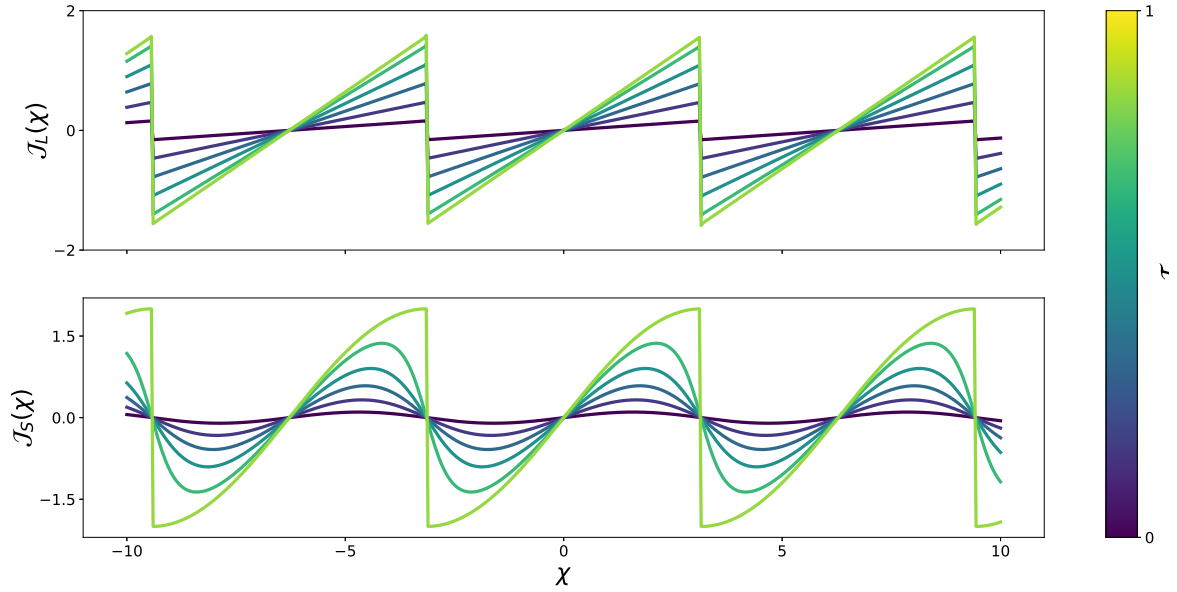


Figure 2.2: Short and long junction current density

\mathcal{T} is the transmission coefficient that describes the transmission through a channel (each channel corresponds to a eigenvalue of the scattering matrix). The current density for the long junction limit is

$$\mathcal{J}(\chi) = \sum_{k=1}^{\infty} \frac{(-1)^{k+1}}{k} \sin(k\chi). \quad (2.7)$$

Figure 2.2 shows a plot of both short and long junction limit current densities. They differ for a large transmission coefficient $\mathcal{T} \simeq 1$, where in the long junction limit we observe a sawtooth like shape and in the short junction limit we have a sinusoidal shape.

Using the current density the Josephson current at zero magnetic field ($\phi = 0$) can be expressed as

$$J(\chi, \phi = 0) = \frac{2ev_F}{\pi\lambda_F L^2} \int_{-W/2}^{W/2} dy_1 dy_2 \frac{\mathcal{J}(\chi)}{\left[1 + \left(\frac{y_1 - y_2}{L}\right)^2\right]^2} \quad (2.8)$$

Including magnetic field

So far, the current has been derived for zero magnetic field. If a finite magnetic field is considered, the phase χ will be modified because of two effects. The magnetic phase that will be acquired along a trajectory connecting two points y_1 and y_2 leads to an additional term in the phase. Then again, *the condition of zero screening current in the bulk superconducting region and the limit of $\lambda_L \rightarrow 0$ require the superconducting phase at the interfaces to become functions of y* **TODO: ? Umschreiben!**

Assuming that the London penetration depth is small to zero in the superconducting regions the

following gauge for the vector potential can be used

$$\mathbf{A} = A_y \mathbf{e}_y, \quad A_y = \begin{cases} -Bx, & -L/2 \leq x \leq L/2, \\ -\frac{1}{2}BL|x|, & |x| > L/2 \end{cases} \quad (2.9)$$

The gauge in eq. (2.9) will give no additional contribution to the phase on straight trajectories

$$\delta\chi = \frac{2\pi}{\Phi_0} \int d\mathbf{l} \cdot \mathbf{A} \quad (2.10)$$

$$= \frac{2\pi}{\Phi_0} \int_{-L/2}^{L/2} \frac{dx}{\cos\theta} A_y(x) \sin\theta \quad (2.11)$$

$$= -\frac{2\pi B}{\Phi_0} \frac{y_2 - y_1}{L} \int_{-L/2}^{L/2} x dx \quad (2.12)$$

$$= 0 \quad (2.13)$$

and therefore, the only contribution to the magnetic phase is

$$\delta\chi = -\frac{\pi\phi(y_1 + y_2)}{W} \Leftrightarrow \tilde{\chi}(y_1, y_2) = \chi - \frac{\pi\phi(y_1 + y_2)}{W}. \quad (2.14)$$

This mean that the current phase relation in the expression for the Josephson current from eq. (2.8) for zero magnetic field has to be replaced by the effective phase $\chi \rightarrow \tilde{\chi}(y_1, y_2)$ and then reads

$$J(\chi, \phi) = \frac{2ev_F}{\pi\lambda_F L^2} \int \int_{-W/2}^{W/2} dy_1 dy_2 \frac{\mathcal{J}(\tilde{\chi}(y_1, y_2))}{\left[1 + \left(\frac{y_1 - y_2}{L}\right)^2\right]^2} \quad (2.15)$$

By maximizing the Josephson current with respect to χ , the critical current can be found:

$$I_c(\phi) = \max_{\chi} \{J(\chi, \phi)\} \quad (2.16)$$

Dependence on W/L ratio? Plot of current?

2.3 Calculation of QPC current

TODO: what happens when a constriction is on top of normal layer, fermi levels etc

The quasiclassical formalism can even be employed to modified SNS junctions. One can build gates on top of the normal region of the junction in a way that the current cannot pass through the gated regions. In the quasiclassical picture this means that the possibilities for trajectories connecting two points at the superconducting interfaces are limited through the geometry of the constriction.

Figure 2.3 shows a schematic of the quantum point contact setup which will be analysed with the quasiclassical formalism. The normal region of the SNS junction is covered by a gate in the middle that has a small split in the middle. The split is located at $(xy) = (0,0)$ so that the sample is symmetric around the origin. The width of the split is in the order of λ_F (**Warum wichtig?**) and can thereby be modelled as an isotropic scattering point with transmission coefficient \mathcal{T}_0 . Consequently, each trajectory connecting the two superconducting interfaces have to pass through the QPC. For simplicity the geometrical width of the barrier is neglected and only straight trajectories (no scattering at side edges) are considered. This modified setup leads first to a different parametrisation of the trajectories and therefore to a different magnetic phase than in

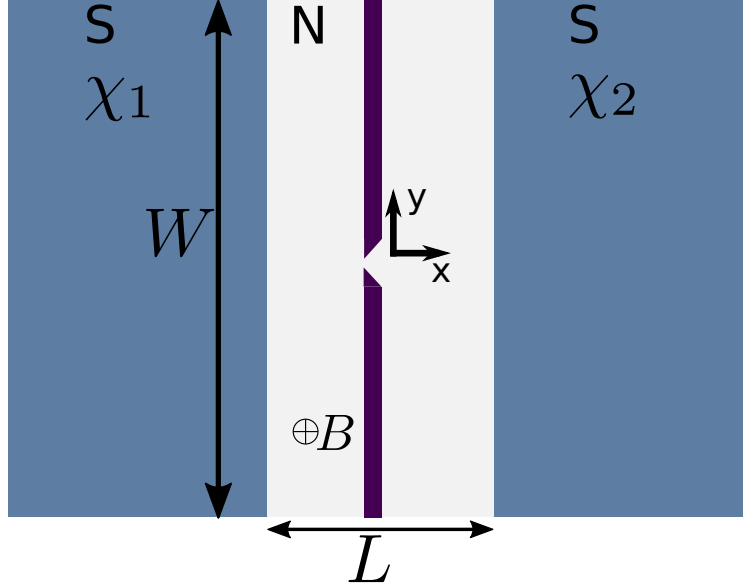


Figure 2.3: QPC setup.

eq. (2.14).

With the QPC setup, all possible trajectories are parametrised by two angles θ_i and θ_f . θ_i describes the trajectory before passing through the QPC in the region $-L/2 < x_0$ and θ_f after passing through the QPC. The parametrisation of the trajectories reads

$$\tan \theta_i = -\frac{2y_i}{L}, \quad \tan \theta_f = \frac{2y_f}{L} \quad (2.17)$$

With the gauge from eq. (2.9) the magnetic phase acquired within the sample reads:

$$\frac{2\pi}{\Phi_0} \int d\mathbf{l} \cdot \mathbf{A} = -\frac{\pi B}{\Phi_0} \left(\frac{L}{2}\right)^2 (-\tan \theta_i + \tan \theta_f) = -\frac{\pi \phi (y_i + y_f)}{2W}. \quad (2.18)$$

Therefore the effective phase is

$$\tilde{\chi}(y_i, y_f) = \chi - \frac{3\pi\phi}{2W}(y_i + y_f). \quad (2.19)$$

The effective phase for the QPC in eq. (2.19) is half of to the effective phase without any constriction, in eq. (2.14). This seems reasonable, since in the QPC setup the all possible straight trajectories can cover only half of the normal region compared to the setup without constriction. The effective phase therefore modifies the current phase relation $\mathcal{J}(\tilde{\chi}(y_i, y_f))$. Beyond that, the expression for the critical current has to be modified as well.

The normalized critical current reads

$$\frac{I_c(\phi)}{I_c(0)} = \frac{\max_{\chi} \int d\theta_i \cos^2 \theta_i \int d\theta_f \cos \theta_f \mathcal{J}(\tilde{\chi}(\theta_i, \theta_f))}{\max_{\chi} \int d\theta_i \cos^2 \theta_i \int d\theta_f \cos \theta_f \mathcal{J}(\chi)} \quad (2.20)$$

In the limit of small transmission probability $\mathcal{T} \ll 1$ we use Eq. (??) for the partial Josephson current. The normalized critical current can then be written as

$$\frac{I_c(\phi)}{I_c(0)} = \frac{\mathcal{I}_2(\phi) \mathcal{I}_{3/2}(\phi)}{\mathcal{I}_2(0) \mathcal{I}_{3/2}(0)} \quad (2.21)$$

The integrals \mathcal{I} are here defined as

$$\mathcal{I}_k(\phi) = \frac{2}{L} \int_{-W/2}^{+W/2} dy \frac{\cos\left(\frac{3\pi\phi y}{2W}\right)}{\left[1 + \left(\frac{2y}{L}\right)^2\right]^k} \quad (2.22)$$

At $\phi = 0$ we get

$$\mathcal{I}_2(0)\mathcal{I}_{3/2}(0) = \frac{L}{\sqrt{L^2 + W^2}} \arctan \frac{W}{L} + \frac{L^2 W}{(L^2 + W^2)^{3/2}} \quad (2.23)$$

The parabolic asymptotics of the critical current at small ϕ is found by expanding the cosine factors in the numerator:

$$\frac{I_c(\phi)}{I_{c0}} \simeq 1 - \frac{9\pi^2\phi^2}{32} f_0(W/L) \quad (2.24)$$

$$f_0(x) = \frac{\sqrt{x^2 + 1} \log(\sqrt{x^2 + 1} + x)}{x} - \frac{x}{x + (x^2 + 1) \arctan(x)} \quad (2.25)$$

In the opposite limit of high fields, $\phi \rightarrow \infty$, we extend the integration in Eq. (2.22) over y_i and y_f to $\pm\infty$ and obtain

$$\frac{I_c(\phi)}{I_{c0}} \simeq \frac{\pi^3}{8x^2} \left(\frac{3\phi}{2x}\right)^{3/2} \frac{(1+x^2)^{3/2}}{x + (1+x^2) \arctan x} \exp\left(-\frac{3\phi\pi}{2x}\right) \quad (2.26)$$

change in magnetic phase, geometrical argument, change in current, limits etc.